MADRID
inter.noise 2019
June 16 - 19
NOISE CONTROL FOR A BETTER ENVIRONMENT

WAVE SCATTERING IN COUPLED COMPOSITE PLATES

Aimakov, Nurkanat[1]
School of Mechanical Engineering
University of Nottingham, Nottingham, NG7 2RD, UK

Tanner, Gregor[2]
School of Mathematical Sciences
University of Nottingham, Nottingham, NG7 2RD, UK

Chronopoulos, Dimitrios[3]
Institute for Aerospace Technology,
University of Nottingham, Nottingham, NG7 2TU, UK

ABSTRACT

Establishing the wave propagation characteristics at plate junctions is of great importance in the prediction of vibrational energy transmission across complex structures. A hybrid approach combining the finite element (FE) and the wave finite element (WFE) method at interconnects between flat, isotropic plates has recently been established for calculating reflection and transmission coefficients. The method is based on modelling joints such as an L-shaped joint with FE with boundary conditions given by the solutions of the WFE method for the infinite plate. We extend this method to study two dimensional anisotropic plates. Numerical results for the bending wave transmission across coplanar and L-shaped junctions are presented. Comparisons of numerically predicted scattering coefficients with analytical solutions for selected structures are used to validate the model. The results obtained are important for Statistical Energy Analysis (SEA) and Dynamical Energy Analysis (DEA) based calculations of wave energy distribution of the full structure.

Keywords: structure-borne sound, wave and finite element method, composites
I-INCE Classification of Subject Number: 43

[1] nurkanat.aimakov@nottingham.ac.uk
[2] gregor.tanner@nottingham.ac.uk
[3] dimitrios.chronopoulos@nottingham.ac.uk

1. INTRODUCTION

Knowledge of wave propagation characteristics such as dispersion relations and scattering coefficients at discontinuities in composite structures is of great importance for many engineering applications. Examples include structural health monitoring and passive noise control. In the simple case of isotropic materials, the analytical models describing dynamic vibro-acoustic behaviour of such structures can be found in [1,2]. However, when the structure is more complicated, for example, anisotropic layered plates, the analytical solutions then become very difficult to obtain at best. In such cases, numerical methods can be exploited. Finite Element Method (FEM) being the most commonly used tool for vibration analysis of complex structures becomes inappropriate when high frequency excitation is applied. This is due to impractically high computational costs.

The Wave Finite Element (WFE) method was originally proposed by Mead [3] as a technique to study wave motion in periodic structures. For such structures, the dynamic vibro-acoustic behaviour of the whole structure can be described through the analysis of a single periodic segment [4]. Huge contribution to the analysis of wave propagation in various periodic structures using a FE model of a single periodic section has been made by Abdel-Rahman [5]. Dispersion curves for thin-walled structures, laminated plates and fluid filled pipes were obtained using WFE method in [6,7,8].

Concerning the computation of scattering coefficients, the simple cases of isotropic plate junctions, plate/beam junctions and curved plates were modelled analytically using wave approaches in [2] and [9,10] by Langley and Heron. The hybrid FE/WFE method for calculating reflection and transmission coefficients was firstly introduced by Mencik and Ichchou for one-dimensional waveguides coupled longitudinally [11]. In recent years, the method has been developed and extended to other types of junctions [12] and to two-dimensional waveguides [13]. However, structures considered in those works were mostly isotropic or were consisting of layers of isotropic materials. In this paper, we extend the hybrid FE/WFE method to composite two-dimensional waveguides.

The paper is organised as follows. In section 2 the WFE method for plates is reviewed. The hybrid FE/WFE method for computation of scattering coefficients in coupled plates is presented in section 3. Some numerical examples and their comparison to the analytical results are presented in section 4. Finally, conclusions are made in section 5.

2. WFE METHOD FOR TWO-DIMENSIONAL WAVEGUIDES

As it was mentioned above, in the WFE method a periodic segment can be used for modelling the dynamic response of the whole periodic structure. Therefore, the size of the WFE model does not depend on dimensions of the waveguide and the computational cost of the method is low. For the sake of simplicity, consider a periodic element of an orthotropic plate which principal material directions coincide with coordinate directions as one presented in Figure 1. The periodic element is modelled using a rectangular three-dimensional finite element with 3 translational degrees of freedom (DOF) per node with dimensions $\mathbf{L_x}$, $\mathbf{L_y}$ and $\mathbf{L_z}$. In commercial FE software such as Ansys SOLID185 can be used for this purpose. Note that higher order finite elements with internal nodes may be used, however, the form of eigenvalue problem sought is reducible to the case without internal nodes via static or dynamic condensation (see [7] for details). The segment can be meshed through its thickness using any number of elements, here we use only one

element for simplicity. Assuming time-harmonic dependence of the form $e^{i\omega t}$ and no external forces, one can write governing equations of motion in the following form:

$$[\mathbf{K} + \mathrm{i}\omega\mathbf{C} - \omega^2\mathbf{M}]\mathbf{q} = \mathbf{f} \tag{1}$$

where $\mathbf{K}$, $\mathbf{C}$ and $\mathbf{M}$ are stiffness, damping and mass matrices respectively, $\mathbf{q}$ and $\mathbf{f}$ are vectors of nodal displacements and forces which are of the following form:

$$\mathbf{q} = \begin{bmatrix} \mathbf{q_1} \\ \mathbf{q_2} \\ \vdots \\ \mathbf{q_8} \end{bmatrix} \quad , \quad \mathbf{f} = \begin{bmatrix} \mathbf{f_1} \\ \mathbf{f_2} \\ \vdots \\ \mathbf{f_8} \end{bmatrix}$$

The harmonic plane waves travelling in some direction θ possess two components $k_x = k\cos\theta$ and $k_y = k\sin\theta$ of the wavenumber k. Note that the wavenumber k depends on the angle of propagation as well as its components in contrast to the isotropic material case. Assuming free wave propagation, one can impose the periodicity condition in the y direction to reduce the dimension of the problem. Specifically, according to the node numbering convention in Figure 1, we can define a transfer matrix $\mathbf{T}$ which relates the full vector of displacements to a reduced set as

$$\begin{Bmatrix} \mathbf{q_1} \\ \mathbf{q_2} \\ \vdots \\ \mathbf{q_8} \end{Bmatrix} = \mathbf{T}\begin{Bmatrix} \mathbf{q_1} \\ \mathbf{q_2} \\ \mathbf{q_3} \\ \mathbf{q_4} \end{Bmatrix} = \mathbf{T}\mathbf{q}_{\mathrm{red}} \quad \text{where} \quad \mathbf{T} = \begin{pmatrix} \mathbf{I} & \mathbf{0} & & \\ \mathbf{0} & \mathbf{I} & \mathbf{0} & \\ & \mathbf{0} & \mathbf{I} & \mathbf{0} \\ & & \mathbf{0} & \mathbf{I} \\ \boldsymbol{\lambda_y}\mathbf{I} & \mathbf{0} & & \\ \mathbf{0} & \boldsymbol{\lambda_y}\mathbf{I} & \mathbf{0} & \\ & \mathbf{0} & \boldsymbol{\lambda_y}\mathbf{I} & \mathbf{0} \\ & & \mathbf{0} & \boldsymbol{\lambda_y}\mathbf{I} \end{pmatrix} \tag{2}$$

where $\mathbf{I}$ is a 3-by-3 identity matrix and $\boldsymbol{\lambda_y} = \boldsymbol{e}^{-i\mathbf{k}_y \mathrm{L}_y}$ – the propagation factor in the y direction. Hence, Equation 1 can be written in terms of the reduced DOFs as

$$\tilde{\mathbf{D}}\mathbf{q}_{\mathrm{red}} = \mathbf{f}_{\mathrm{red}} \quad , \quad \text{where} \quad \tilde{\mathbf{D}} = \mathbf{T}^H[\mathbf{K} + \mathrm{i}\omega\mathbf{C} - \omega^2\mathbf{M}]\mathbf{T} \quad \text{and} \quad \mathbf{f}_{\mathrm{red}} = \mathbf{T}^H\mathbf{f} \tag{3}$$

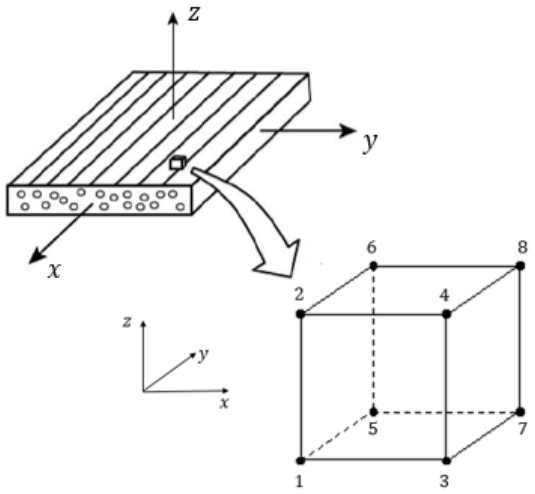

Figure 1: Segment of an orthotropic plate and its periodic element with node numbering convention.

One can decompose the vector of nodal displacements and forces into parts associated with left and right cross sections so that Equation 3 can be rewritten as

$$\begin{bmatrix} \widetilde{\mathbf{D}}_{\mathbf{LL}} & \widetilde{\mathbf{D}}_{\mathbf{LR}} \\ \widetilde{\mathbf{D}}_{\mathbf{RL}} & \widetilde{\mathbf{D}}_{\mathbf{RR}} \end{bmatrix} \begin{Bmatrix} \mathbf{q}_{\mathbf{L}} \\ \mathbf{q}_{\mathbf{R}} \end{Bmatrix} = \begin{Bmatrix} \mathbf{f}_{\mathbf{L}} \\ \mathbf{f}_{\mathbf{R}} \end{Bmatrix} \tag{4}$$

where $\mathbf{q}_{\mathbf{L}} = \begin{Bmatrix} \mathbf{q}_1 \\ \mathbf{q}_2 \end{Bmatrix}$ and $\mathbf{q}_{\mathbf{R}} = \begin{Bmatrix} \mathbf{q}_3 \\ \mathbf{q}_4 \end{Bmatrix}$. The vector of nodal forces is arranged in the same manner. The form of the equation of motion obtained is identical to the one in the case of one-dimensional waveguides [12], only now the problem is reduced and all partitioned parts of the dynamic stiffness matrix $\widetilde{\mathbf{D}}$ depend on the component $\mathbf{k}_y$ of the wavenumber $\mathbf{k}$ to which one would need to set some fixed values. Further, utilising the periodicity conditions now in the x direction which can be written as

$$\mathbf{q}_{\mathbf{R}} = \boldsymbol{\lambda}_x \cdot \mathbf{q}_{\mathbf{L}} \ , \ \mathbf{f}_{\mathbf{R}} = - \boldsymbol{\lambda}_x \cdot \mathbf{f}_{\mathbf{L}} \tag{5}$$

one can get the following eigenvalue problem for the unknown wave propagation constant $\boldsymbol{\lambda}_x$

$$\mathbf{T} \begin{Bmatrix} \mathbf{q}_{\mathbf{L}} \\ \mathbf{f}_{\mathbf{L}} \end{Bmatrix} = \lambda_x \begin{Bmatrix} \mathbf{q}_{\mathbf{L}} \\ \mathbf{f}_{\mathbf{L}} \end{Bmatrix} \text{ where } \mathbf{T} = \begin{bmatrix} -\mathbf{D}_{\mathbf{LR}}^{-\mathbf{1}}\mathbf{D}_{\mathbf{LL}} & \mathbf{D}_{\mathbf{LR}}^{-\mathbf{1}} \\ -\mathbf{D}_{\mathbf{RL}} + \mathbf{D}_{\mathbf{RR}}\mathbf{D}_{\mathbf{LR}}^{-\mathbf{1}}\mathbf{D}_{\mathbf{LL}} & -\mathbf{D}_{\mathbf{RR}}\mathbf{D}_{\mathbf{LR}}^{-\mathbf{1}} \end{bmatrix} \tag{6}$$

is the transfer matrix. However, this form of the eigenvalue problem may suffer from ill-conditioning when the number of DOFs is high which regularly appear to be the case for anisotropic composite plates. Therefore, we used an alternative form of the eigenvalue problem which is based on symplectic properties of the transfer matrix (see [14,15] for details). Regardless of the eigenvalue problem posed, one can find the unknown x-components $\mathbf{k}_x$ of the wavenumber $\mathbf{k}$ by using computed eigenvalues $\boldsymbol{\lambda}_x$ so that wave dispersion curves can be drawn.

Since the transfer matrix is symplectic, the set of eigenvalues can be divided into reciprocal pairs as λ_j^+ and $\lambda_j^- = 1/\lambda_j^+$ with wavenumbers $k_j^+ = \frac{\log(\lambda_j^+)}{-i\mathbf{L}_\mathbf{x}}$ and $k_j^- = -k_j^+$ corresponding to positive-going and negative-going waves respectively [7]. The eigenvectors $\phi_j^{\pm} = \begin{Bmatrix} \phi_{\mathbf{q}}^{\pm} \\ \phi_{\mathbf{f}}^{\pm} \end{Bmatrix}_j$ contain information about nodal displacements and forces under the propagation of the correspondent wave. These eigenvectors are called wave modes. The nodal displacements and forces can be expressed as a linear combination of the wave modes with amplitudes a_j (see Equation 7).

$$\begin{bmatrix} \mathbf{q} \\ \mathbf{f} \end{bmatrix} = \sum_{j=1}^{8} \left(a_j^+ \begin{bmatrix} \phi_{\mathbf{q,j}}^+ \\ \phi_{\mathbf{f,j}}^+ \end{bmatrix} + a_j^- \begin{bmatrix} \phi_{\mathbf{q,j}}^- \\ \phi_{\mathbf{f,j}}^- \end{bmatrix} \right) = \begin{bmatrix} \mathbf{\Phi}_{\mathbf{q}}^+ \mathbf{a}^+ + \mathbf{\Phi}_{\mathbf{q}}^- \mathbf{a}^- \\ \mathbf{\Phi}_{\mathbf{f}}^+ \mathbf{a}^+ + \mathbf{\Phi}_{\mathbf{f}}^- \mathbf{a}^- \end{bmatrix} \tag{7}$$

3. HYBRID FE/WFE METHOD AND SCATTERING COEFFICIENTS

In this section, we show how to compute the reflection/transmission coefficients of joints of finite size by using hybrid FE/WFE method. Basically, the method consists in modelling plates using WFE and the coupling element – using standard finite elements (see Figure 2). Then, by imposing continuity and equilibrium conditions at interfaces, one

can compute the scattering matrix $\mathbf{s}$ – the matrix which relate the amplitudes of incoming and outgoing waves as

$$\begin{Bmatrix}\mathbf{a}_1^- \\ \mathbf{a}_2^-\end{Bmatrix} = \mathbf{s}\begin{Bmatrix}\mathbf{a}_1^+ \\ \mathbf{a}_2^+\end{Bmatrix} \quad , \quad \mathbf{s} = \begin{bmatrix}\mathbf{r_{11}} & \mathbf{t_{12}} \\ \mathbf{t_{21}} & \mathbf{r_{22}}\end{bmatrix} \tag{8}$$

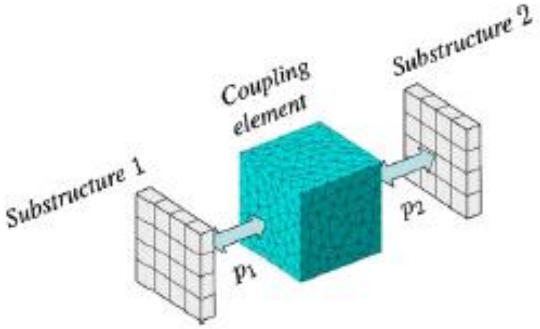

Figure 2: A hybrid FE/WFE problem. Picture taken from [16].

The governing equation of the coupling element can be written as

$$\begin{bmatrix}\widetilde{\mathbf{D}}_{ii} & \widetilde{\mathbf{D}}_{in} \\ \widetilde{\mathbf{D}}_{ni} & \widetilde{\mathbf{D}}_{nn}\end{bmatrix}\begin{Bmatrix}\mathbf{Q}_i \\ \mathbf{Q}_n\end{Bmatrix} = \begin{Bmatrix}\mathbf{F}_i \\ \mathbf{F}_n\end{Bmatrix} \tag{9}$$

where nodes at the interfaces between the plates and the joint are denoted by i whereas non-interface nodes - by n. Assuming no external forces on the non-interface nodes, Equation 9 can be reduced to the form with only interface nodes involved via static or dynamic condensation. Imposing continuity of nodal displacements and equilibrium of nodal forces at the interfaces between the plates and the joint as

$$\begin{aligned}\mathbf{Q}_i &= \mathbf{R}\left[\boldsymbol{\Phi}_{\boldsymbol{Q}}^{+}\begin{Bmatrix}\boldsymbol{a}_1^+ \\ \boldsymbol{a}_2^+\end{Bmatrix} + \boldsymbol{\Phi}_{\boldsymbol{Q}}^{-}\begin{Bmatrix}\boldsymbol{a}_1^- \\ \boldsymbol{a}_2^-\end{Bmatrix}\right] \quad , \quad \boldsymbol{\Phi}_{\boldsymbol{Q}}^{\pm} = \begin{bmatrix}\boldsymbol{\Phi}_{\mathbf{q}}^{\mathbf{1}\pm} & \mathbf{0} \\ \mathbf{0} & \boldsymbol{\Phi}_{\mathbf{q}}^{\mathbf{2}\pm}\end{bmatrix} \\ \mathbf{F}_i &= \mathbf{R}\left[\boldsymbol{\Phi}_{\boldsymbol{F}}^{+}\begin{Bmatrix}\boldsymbol{a}_1^+ \\ \boldsymbol{a}_2^+\end{Bmatrix} + \boldsymbol{\Phi}_{\boldsymbol{F}}^{-}\begin{Bmatrix}\boldsymbol{a}_1^- \\ \boldsymbol{a}_2^-\end{Bmatrix}\right] \quad , \quad \boldsymbol{\Phi}_{\boldsymbol{F}}^{\pm} = \begin{bmatrix}\boldsymbol{\Phi}_{\mathbf{f}}^{\mathbf{1}\pm} & \mathbf{0} \\ \mathbf{0} & \boldsymbol{\Phi}_{\mathbf{f}}^{\mathbf{2}\pm}\end{bmatrix}\end{aligned} \tag{10}$$

yields an expression for the scattering matrix as

$$\mathbf{s} = -\left[\mathbf{D}_{ii}\,\mathbf{R}\boldsymbol{\Phi}_{\boldsymbol{Q}}^{-} - \mathbf{R}\boldsymbol{\Phi}_{\boldsymbol{F}}^{-}\right]^{-1}\left[\mathbf{D}_{ii}\,\mathbf{R}\boldsymbol{\Phi}_{\boldsymbol{Q}}^{+} - \mathbf{R}\boldsymbol{\Phi}_{\boldsymbol{F}}^{+}\right] \tag{11}$$

where $\mathbf{R} = \begin{bmatrix}\mathbf{R_1} & \mathbf{0} \\ \mathbf{0} & \mathbf{R_2}\end{bmatrix}$ – rotation matrix which transform the nodal displacements and forces from local coordinate systems of plates to the global one. If the inverse transformation in Equation 11 cannot be applied due to the singularity of the matrix considered, then one can use a pseudoinverse via singular value decomposition. Note that the scattering matrix $\mathbf{s}$ depends on the angular frequency ω and on the angle of incidence θ via $\tan\theta = \frac{\mathbf{k}_y}{\mathbf{k}_x}$.

4. NUMERICAL EXAMPLES

Several example applications are presented in this section. Coplanar coupled isotropic plates are considered in the first example. Scattering coefficients for an L-junction of isotropic plates are computed numerically and compared with analytical ones in the next example. Finally, an example of an L-junction of orthotropic plates is given. The choice of the first two numerical examples was motivated by the existence of analytical expressions for dispersion curves and scattering coefficients.

4.1. Coplanar coupled isotropic plates

In our first example we consider two isotropic plates coupled along the x-axis as shown in Figure 3. Plates have different material properties but same thicknesses (see Table 1).

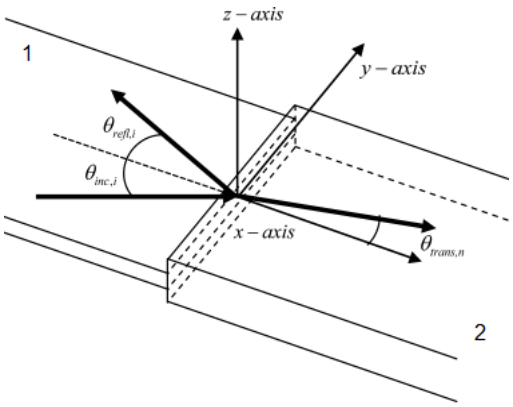

Figure 3 : Coplanar coupled plates. A plane wave impinges on a junction of plates 1 and 2 and gives rise to reflected and transmitted waves.

	Plate 1	Plate 2
Young Modulus E	207 GPa	71.0 GPa
Poisson's ratio ν	0.3	0.28
Density ρ	$7800\,\mathrm{kg/m^3}$	$2700\,\mathrm{kg/m^3}$
Thickness h	0.003	0.003

Table 1 : Material parameters of isotropic plates.

In Figure 4 power scattering coefficients with respect to the angle of incidence computed for an incident bending wave at the frequency $\mathrm{f} = 3$ kHz are presented. There is no mode conversion into other wave types such as shear or pressure. One can notice that for all angles of incidence, the incident power is mainly transmitted to the second plate. Numerical results show a very good agreement with the semi-analytical results obtained from the work of Langley and Heron [9]. Furthermore, the fact that the sum of power reflection and transmission coefficients is equal to unity ensures the validity of results obtained.

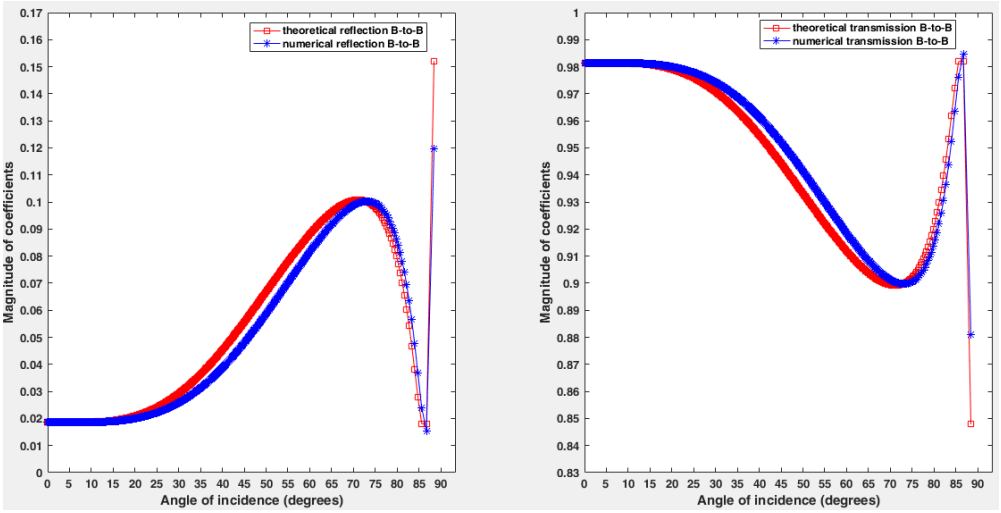

Figure 4 : Reflection and transmission coefficients of the incident bending wave in coplanar coupled plates at the frequency f = 3 kHz.

4.2. L-junction of isotropic plates

In this example, the structure is comprised of two identical isotropic plates with material parameters as of the plate 2 in the previous example. Plates are coupled at 90 degrees as shown in Figure 5.

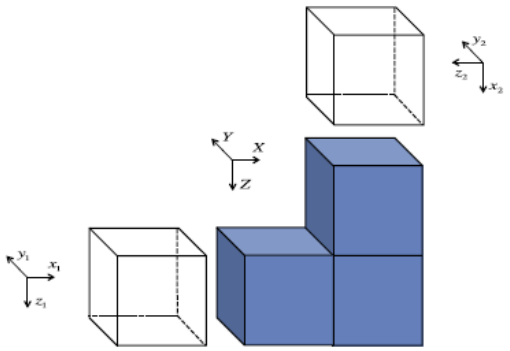

Figure 5 : Two periodic elements of an isotropic plate are coupled with L-shaped joint. Figure is taken from [13].

Figure 6 shows how the power scattering coefficients of an incident bending wave vary with respect to the angle of incidence at the frequency f = 3 kHz. One can investigate the mode conversion phenomenon: an incident bending wave gives rise not only to bending reflected or transmitted waves but also to pressure and shear waves. However, this phenomenon is observed up to some angles which are known as critical angles. In the top right plot, one can notice that at angles higher than 3 degrees reflection and transmission from bending to pressure (B-to-P) are equal to zero. The critical angle of the bending to shear mode conversion (B-to-SH) is around 5 degrees (see the bottom right plot). At normal incidence, e.g. $\theta = 0^{\circ}$, the power is almost equally distributed between reflected and transmitted waves. Note that at critical angles for pressure and shear waves, reflection and transmission of the bending to bending type (B-to-B) undergo a change by which their values are decreasing or increasing instantly. As shown in Figure 6, the numerical results are in a good agreement with the semi-analytical ones from [9]. However, for higher frequencies the difference between numerical and analytical results increases (see Figure 7).

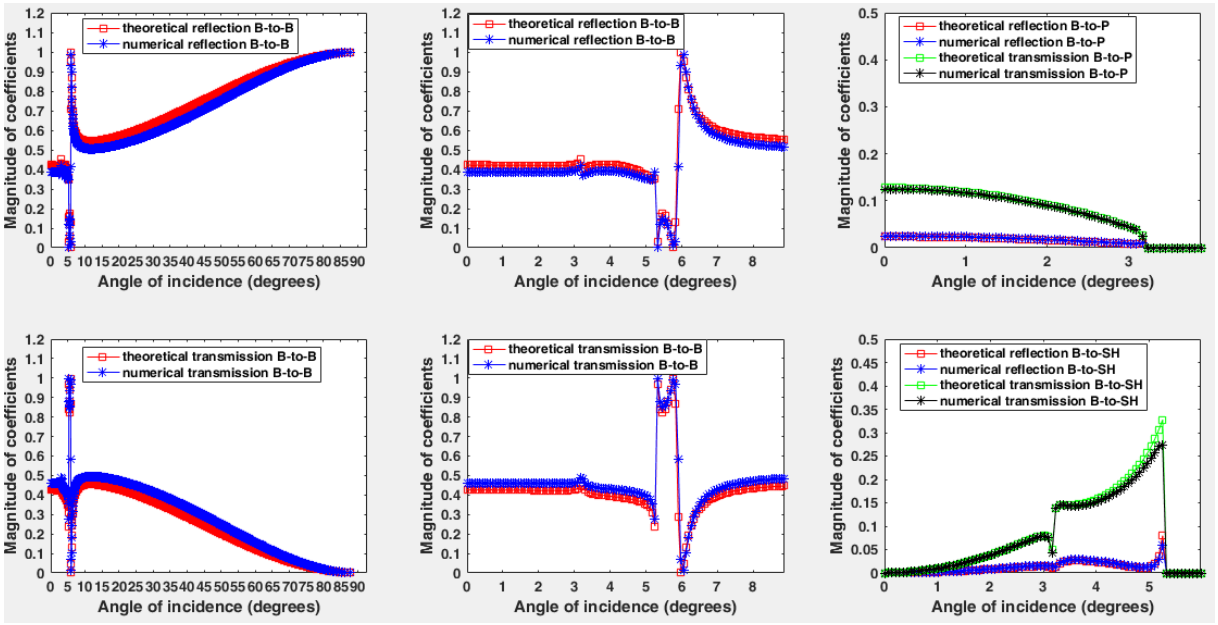

Figure 6 : Power scattering coefficients for an incident bending wave in L-shaped isotropic plates at frequency $f = 3\ kHz$, dimensionless wavenumber value $k_b h = 0.19$.

This can be referred to the fact that we used the analytical model based on the assumption that the joint can be represented as a shared line between plates. This assumption breaks down at higher frequencies since the influence of the joint size becomes larger. Particularly, the shear strain becomes more important on the dynamic response of the joint and this effect is not considered in the analytical model (see [17] for details). Nevertheless, the summation to unity of the power reflection and transmission coefficients validates the results obtained.

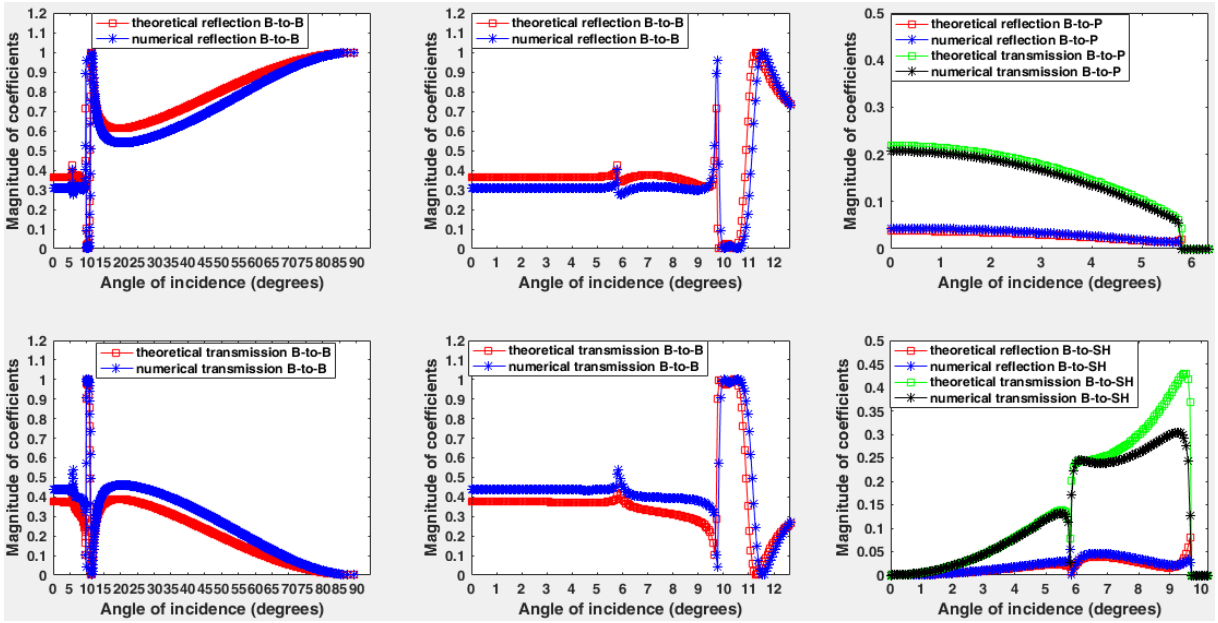

Figure 7: Power scattering coefficients for an incident bending wave in L-shaped isotropic plates at frequency $f = 10\ kHz$, dimensionless wavenumber value $k_b h = 0.35$.

4.3. L-junction of orthotropic plates

Finally, an L-junction of two identical orthotropic plates is considered (see Figure 8). The material parameters chosen are presented in Table 2.

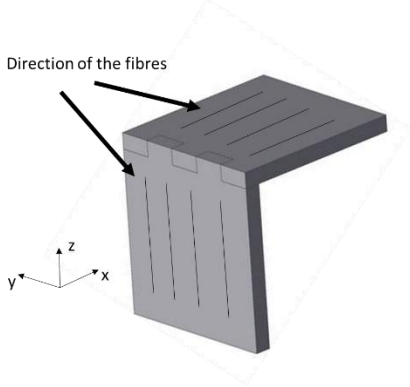

Figure 8: L-junction of two orthotropic plates.

E_x	127 GPa
$E_y = E_z$	11.3 GPa
$\nu_{xy} = \nu_{xz}$	0.3
ν_{yz}	0.34
$G_{xy} = G_{xz}$	5.97 GPa
G_{yz}	3.75 GPa
ρ	$1578\,\mathrm{kg/m^3}$
Thickness h	0.003

Table 2: Material parameters of the orthotropic plate.

Figure 9 demonstrates the polar dispersion curves obtained for an orthotropic thin plate at the frequency f = 3 kHz. Note that the total wavenumber of retained waves depends on the angle of propagation. A very good agreement is observed between theoretical dispersion curves based on the Kirchhoff-Love plate theory and the ones obtained with WFE. These numerical dispersion relations can be used to calculate the group velocity angles and therefore propagation angles of transmitted waves via modified Snell's law.

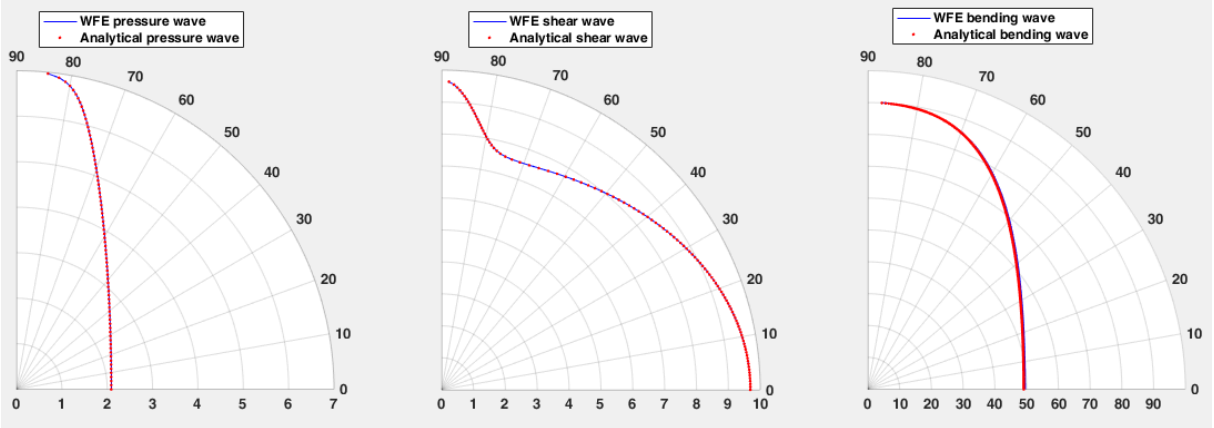

Figure 9: Polar dispersion curves of the orthotropic thin plate at the frequency $f = 3\ kHz$. Angle of propagation varies between 0 and 90 degrees.

In Figure 10, the power scattering coefficients for the incident bending wave at the frequency $f = 3\ kHz$ are plotted. At almost all angles of incidence, more than a half of the incident power is reflected to the first plate. At the critical angle for shear waves $\theta \approx 12^{\circ}$, the transmitted power instantly increases up to 90 percent of the incident power and then drops down after a small angle increment which appears to be odd, however, the overall behaviour of curves is like the one in the case of L-junction of isotropic plates (see Figure 6 and 7). A slightly different behaviour of power scattering coefficients is observed at higher frequencies (see Figure 11). At low angles of incidence, B-to-B reflected and transmitted power ratios do not change a lot, instead values of the scattering coefficients B-to-P and B-to-SH are increased. The critical angles for pressure and shear waves are higher than in the low frequency case. Also, around 80 percent of incident power is reflected to the first plate at angles higher than the critical angle for shear waves $\theta \approx 20^{\circ}$. Note that the power reflection and transmission coefficients sum up to unity at all angles of incidence.

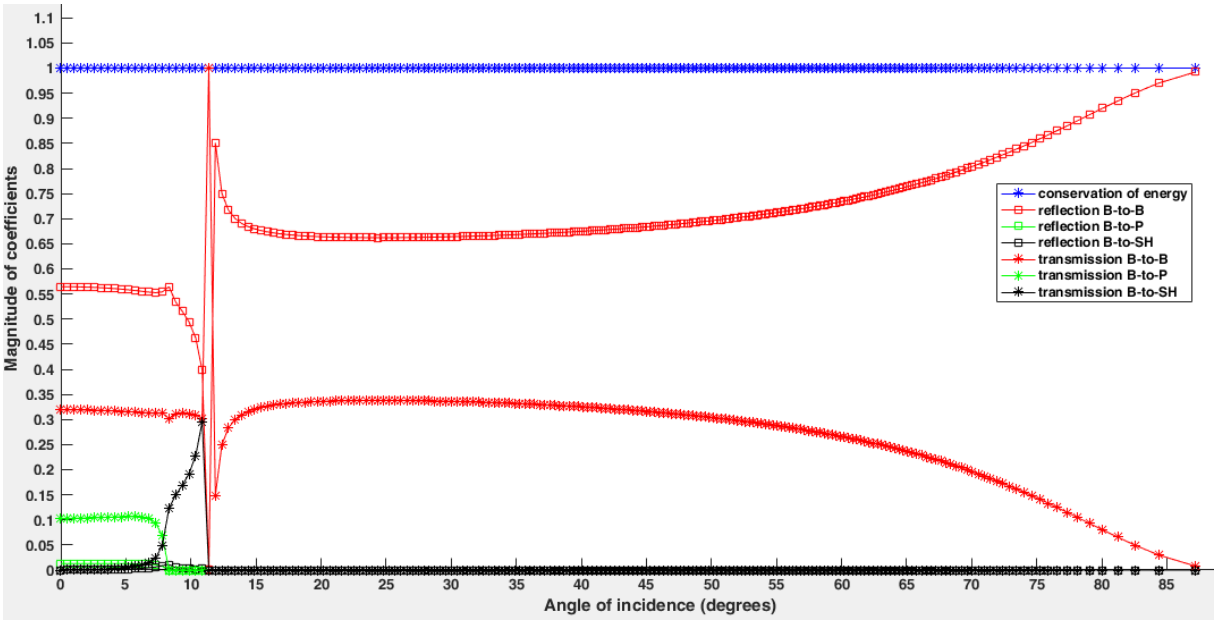

Figure 10: Power scattering coefficients for an incident bending wave in L-shaped orthotropic plates at frequency $f = 3\ kHz$*, dimensionless wavenumber value* $k_b h = 0.19$.

4. CONCLUSION

A hybrid FE/WFE model that predicts the scattering properties for different junctions of two-dimensional isotropic and anisotropic composite plates has been developed. The influence of the angle of incidence and of the frequency on the distribution of the power flow of incident bending type waves has been investigated. The results of this paper can be used for the computation of wave energy distribution in Statistical and Dynamical Energy Analysis.

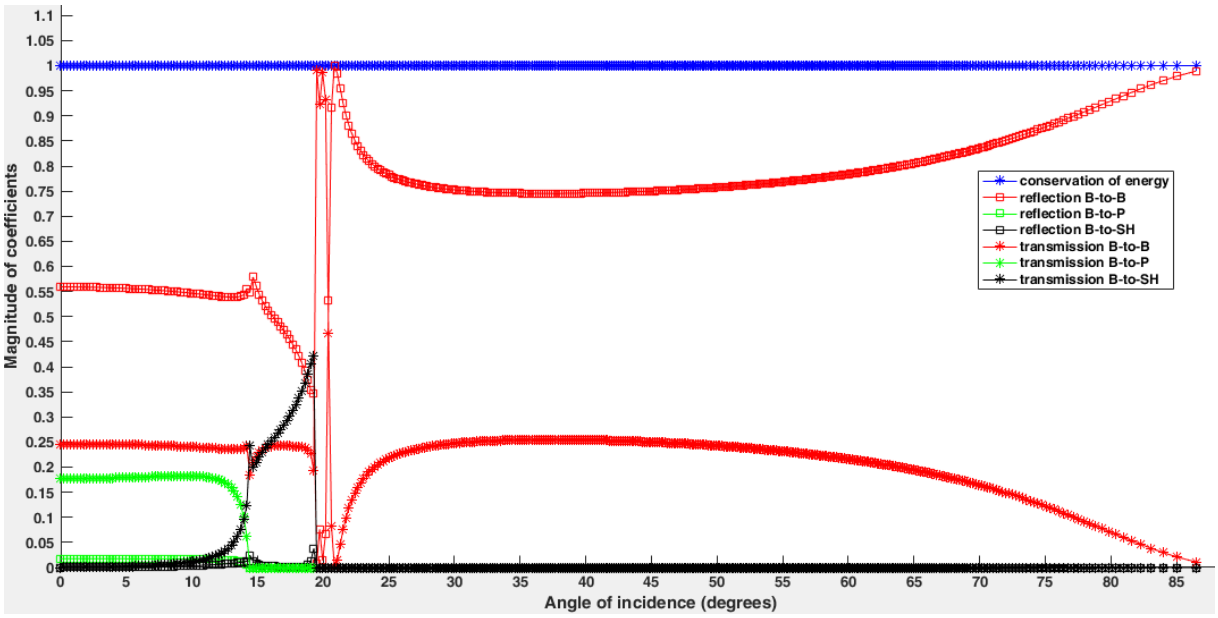

Figure 11: Power scattering coefficients for an incident bending wave in L-shaped orthotropic plates at frequency $f = 10\ kHz$*, dimensionless wavenumber value* $k_b h = 0.5$.

5. ACKNOWLEDGEMENTS

This work is funded by the INNOVATIVE doctoral programme. The INNOVATIVE programme is partially funded by the Marie Curie Initial Training Networks (ITN) action (project number 665468) and partially by the Institute for Aerospace Technology (IAT) at the University of Nottingham.

6. REFERENCES

[1] K.F. Graff. *Wave motion in Elastic Solids*. Oxford University Press, 1975.

[2] L. Cremer, M. Heckl, E.E. Ungar. *Structure-Borne Sound, Second ed.*, Springer, 1973.MARC Analysis Research Corporation. MARC general purpose finite element program. Palo Alto, CA, 1986.

[3] D. J. Mead. A general theory of harmonic wave propagation in linear periodic systems with multiple coupling. Journal of Sound and Vibration, 27, 235-260, 1973.

[4] G. Floquet. Sur les équations différentielles linéaires à coefficients périodiques. Annales scientifiques de l'Ecole Normale Supérieure, 12, 47-88, 1883.

[5] A. Abdel-Rahman. Matrix analysis of wave propagation in periodic systems. PhD thesis, University of Southampton, 1979.

[6] L. Houillon, M. Ichchou, L. Jezequel. Wave motion in thin-walled structures. Journal of Sound and Vibration, 281, 483-507, 2005.

[7] B. R. Mace, D. Duhamel, M. J. Brennan, L. Hinke. Finite element prediction of wave motion in structural waveguides. Journal of Acoustical Society of America, 117 (5), 2005.

[8] M. Maess, N. Wagner, L. Gaul. Dispersion curves of fluid filled elastic pipes by standard fe models and eigenpath analysis. Journal of Sound and Vibration, 296, 264-276, 2006.

[9] R. S. Langley, K. H. Heron. Elastic wave transmission through plate/beam junctions. Journal of Sound and Vibration, 143, 241-253, 1990.

[10] R. S. Langley. Elastic wave transmission coefficients and coupling loss factors for structural junctions between curved panels. Journal of Sound and Vibration, 169 (3), 297-317, 1994.

[11] J. –M. Mencik, M. N. Ichchou. Multi-mode propagation and diffusion in structures through finite elements. European Journal of Mechanics and Solids, 24, 877-898, 2005.

[12] J. M. Renno, B. R. Mace, Calculation of reflection and transmission coefficients of joints using a hybrid finite element/wave and finite element approach, Journal of Sound and Vibration, 332, 2149-2164, 2013.

[13] G. Mitrou, N. Ferguson, J. Renno. Wave transmission through two-dimensional structures by the hybrid FE/WFE approach. Journal of Sound and Vibration, 389, 484-501, 2017.

[14] W. X. Zhong, F. W. Williams. On the direct solution of wave propagation for repetitive structures. Journal of Sound and Vibration, 181 (3), 485-501, 1995.

[15] Y. Fan, M. Collet, M. Ichchou, L.Li, O. Bareille, Z. Dimitrijevic. Energy flow prediction in built-up structures through a hybrid finite element/wave and finite element approach. Mechanical Systems and Signal Processing, 66-67, 137-158, 2016.

[16] M. N. Ichchou, J.-M. Mencik, W. Zhou. Wave finite elements for low and mid-frequency description of coupled structures with damage. Comput. Methods Appl. Mech. Engrg., 198, 1311-1326, 2009.

[17] V. Zalizniak, Y. Tso, L. Wood. Wave transmission through plate and beam junctions. International Journal of Mechanical Sciences, 41 (7), 831-843, 1999.